Digest Journal of Nanomaterials and Biostructures Vol. 17, No. 3, July - September 2022, p. 999 - 1010

Fabrication of Ag/TiO_2 nanotube array as active electrocatalyst for the hydrogen evolution reaction

M. Mîndroiu[a,*], M. Popescu[b]
[a]University POLITEHNICA of Bucharest, Faculty of Applied Chemistry and Materials Science, 1-7 Polizu, 011061, Bucharest, Romania
[b]National Institute for Research and Development in Microtechnologies, 126A, Erou Iancu Nicolae Street, 077190, Bucharest, Romania

Silver nanoparticles (Ag NPs) were fabricated onto titanium substrates with and without titania nanotubes arrays (TiO_2 NTs) using electrochemical and chemical techniques, respectively, to create nanostructured electrocatalysts for the hydrogen evolution reaction (HER). The active surface area of the catalyst is determined by the Ag NPs' structure and the presence of TiO_2 nanotubes on the titanium substrate. The electrocatalytic activity was improved by chemically synthesizing Ag NPs onto a titanium electrode that had been pre-coated with TiO_2 nanotubes.

(Received April 15, 2022; Accepted August 22, 2022)

Keywords: TiO_2 nanotube, Silver nanoparticles, Electrocatalysis,
Hydrogen evolution reaction

1. Introduction

The recent depletion of oil and gas reserves, as well as environmental pollution caused by climate change, has attracted attention in environmentally friendly energy alternatives such as electrochemical water splitting (ECWS), which uses a hydrogen evolution reaction (HER) half-cell to store renewable electricity as hydrogen (H_2) [1, 2]. Hydrogen has been identified as one of the cleanest energy carriers [3-5] and it has been discovered that hydrogen can be used to replace fossil fuels as a source of energy [6, 7]. Hydrogen is produced using a variety of methods, including electrolysis of water, bio-photolysis and biological production from waste organic material [8, 9]. Despite the high energy requirements, hydrogen production by electrolysis or photoelectrolysis of water is regarded an efficient and feasible method for producing hydrogen with no negative environmental consequences [10, 11]. In this method, two half reactions are involved, the one is the oxygen evolution reaction (OER) on the anode side, and the other one is hydrogen evolution reaction (HER) on the cathode side. In order to increase the efficiency of the hydrogen production via electrolysis requires highly active electrocatalysts for HER Highly active electrocatalysts for HER are required to boost the efficiency of hydrogen production via electrolysis [12, 13]. Bockris et al. [14] investigated the HER and various parameters that influence it, such as the type of solution, which can be acidic [15, 16] or alkaline [17, 18], temperature dependence [19], and different materials that can be used as electrocatalysts, such as platinum (Pt), mercury, gold, copper, tungsten, and silver [20, 21]. In order to reduce the overpotential and to promote the hydrogen production, the hydrogen evolution reaction requires an active catalyst. Pt is the most active catalyst for HER in acidic solutions [22], however its commercialization for this process is limited due to low reserve and expensive price. Furthermore, it was discovered that Pt-based cathodes are highly susceptible to poisoning in the presence of small amounts of metal ion impurities, resulting in contamination of the feeding water [24]. As a result, the development of certain cost-effective, more catalytically active site, and stable HER electrocatalysts is required [25].

---

[*] Corresponding author: mihaela.mindroiu@upb.ro

https://doi.org/10.15251/DJNB.2022.173.999

In recent years, nanostructured metal electrocatalysts have been created for HER [26, 27], and it has been demonstrated that even a minor increase in the electrochemical surface enhances catalytic activity [28]. Anodically grown titania (TiO_2) nanotubes (NTs) arrays have been widely studied n-type semiconducting materials for a variety of applications in photo-electrochemical water splitting [29], degradation of organic pollutants [30], catalysis and photo-catalysis [31], energy storage, solar energy conversion [32] due to their low cost, non-toxicity, and their unique self-aligned structure which improves optical properties and one-dimensional electron transport pathways for efficient charge separation [33]. Self-organized TiO_2 nanotubes (NTs) arrays can be produced by anodizing titanium (Ti) substrates in either aqueous or organic solutions [34-36] in the presence of fluoride ions, by varying a few parameters, such as: F^- concentration, anodization time and voltage, pH of the solution [37, 38]. As all TiO_2 cathodes, bare TNs are inactive for the HER because of a low electrical conductivity ($\approx 10^{-12}$ S cm^{-1}) of TiO_2 and due to the wide band gap (3.2 eV for anatase and 3.0 eV for rutile), but, their high surface area and chemical stability in all pH ranges make them attractive as supporting structures for HER nanocatalysts [29]. In recent years, the catalytic activity of the TiO_2 nanotube arrays for HER has been improved by doping with metallic nanostructured co-catalysts such as Mo, Co, Fe, Ni, Ag, Au [39-41], and W of sulfide [42], nitride [43], using various techniques, such as electrodeposition [24], sputtering [44], spin-coating [45], chemical reduction method [46] and photo-deposition [47]. Due to the unique properties (e.g., size and shape depending optical, electrical, and magnetic properties [48], the AgNPs can be used for various applications, such as catalysts [39, 46, 48], antimicrobial applications [49], biosensor materials [50]. Furthermore, the importance of silver-based catalysts in the catalytic removal of environmental contaminants, the production of clean energy and the distillation of fuel has been demonstrated [51].

In this study, we present the chemical and electrochemical synthesis of nanostructured electrocatalysts based silver nanoparticles on Titanium substrate. Furthermore, based on our previous study [35], the titanium substrate was changed by electrochemical anodization to create TiO_2 nanotubes in order to explore the effect of surface morphology on the electrocatalytic activity of the resulting catalysts.

2. Methods and procedure

2.1. Synthesis of catalysts based TiO_2 NTs and Ag NPs

2.1.1. Synthesis of TiO_2 NTs using anodic treatment

Commercially pure Ti foils of 10 mm diameter and 1 mm thickness (99.6% purity – grade 2, Goodfellow Cambridge Ltd., UK) were used. Before any treatment, the surface of titanium electrode was polished with SiC paper to grade 4000 and then cleaned by sonication in deionized water, ethanol and acetone from 10 minutes each, and then dried in air at room temperature. The samples were anodized in ethylene glycol electrolyte containing 0.5 wt% NH_4F and a small amount of deionized water (2 %) at 40V for 2 h. A conventional two-electrode configuration with platinum cathode electrode and Ti anode electrode and a MATRIX MPS-7163 electrochemical source was used. After anodization, the amorphous TiO_2 nanotubes were crystallized into anatase phase by annealing the foil at 500 ºC for 1 h in air. The growth mechanism of TiO_2 nanotube array was already explained in previous works [35, 52].

2.1.2. Electrochemical synthesis of silver nanoparticles (Ag NP_sel)

Silver nanoparticles (Ag NPs) were electrochemical reduction on Ti and Ti/TiO_2NT electrodes from a silver nitrate ($AgNO_3$ 0.1 M, Merck) aqueous solution, used as silver ion precursor. Electrodeposition was carried out by chronoamperometry method, using one compartment cell with three electrodes: Ti or Ti/TiO_2NTs were used as working electrode, a platinum counter-electrode and Ag/AgCl, KCl reference electrode, connected to an Autolab PGSTAT 302N potentiostat with general-purpose electrochemical system software. In order to reveal the optimal potential at which the electrocatalytic activity is the best, the potential value was applied from – 0.8 V to – 1 V for 50 s.

2.1.3. Chemical synthesis of silver nanoparticles (Ag NP_sch)

For chemical synthesis of *$AgNP_s$ch* the Ti and Ti/TiO_2NTs electrodes were simply soaked in an $AgNO_3$ 0.1 M and NH_4F 5 10^{-3} M aqueous solution for 60 min, at room temperature without any per-treatments for substrates. In literature, the influence of the concentration of $AgNO_3$ and of NH_4F solutions, and also, the time immersion of Ti substrate in this mixture, has been already studied [46]. All wet chemical depositions were conducted in the dark, in order to avoid the effect of light on the deposition of *$AgNP_s$ch* on the electrodes surface. Adding of F^- ions into synthesis solution plays an important role in Ag^+ ions reduction to Ag (0) onto Titanium substrate [46]. The Scanning Electron Microscopy (SEM) morphology of the modified titanium surface with *$AgNP_s$* synthesized by chemical method (Figure 1) reveals that the entire surface was uniform covered with Ag NPs aggregations.

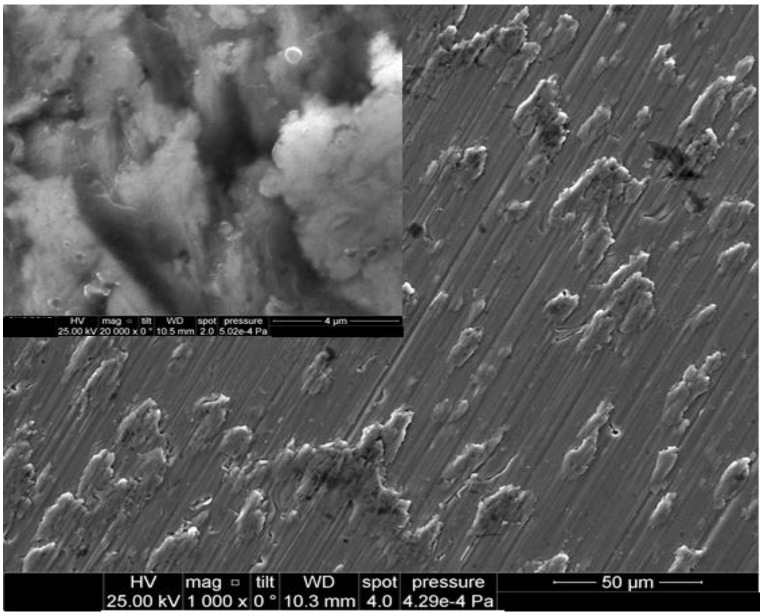

Fig. 1. SEM images of Ag NP chemical deposited on Ti substrate (Ti-AgNPs ch. electrocatalyst).

2.2. Materials Characterization

2.2.1. Physical characterization

The morphology and compositions of Ag NPs supported on Ti and Ti/TiO_2NTs electrodes were achieved by Scaning Electron Microscopy (SEM), using a FEI Nova NanoSEM 630 FEG-SEM (SEM with Field Emission Gun) with ultra-high resolution characterization at high and low voltage in high vacuum. The voltage of SEM analysis was 20 kV and the magnification of the images was between 1000X and 50000X. The elemental composition was investigated using Carl Zeiss Evo 50 XVP scanning electron microscope (SEM) equipped with energy dispersive X-ray analysis (EDAX) Quantax Bruker 200 accessory.

2.2.2. Electrocatalytic activity of synthetized electrocatalysts: Ti-AgNPs el, Ti-AgNPs ch, Ti/TiO_2NTs-AgNPs el, Ti/TiO_2NTs-AgNPs ch

The electrocatalytic activity of the obtained electrocatalysts towards the HER was studied in the test solution (0.1 M HCl), using linear potential sweep voltammetry (LSV) and electrochemical impedance spectroscopy (EIS) methods. LSV technique consisted in obtaining polarization curves scanning the potential towards the negative direction, starting from the corrosion potential (E_{corr}) down to -2 V potential value at a scan rate of 1.0 $mV{\cdot}s^{-1}$. Impedance measurements were performed in the frequency range 0.01 Hz to 100 kHz with an AC voltage amplitude of 5 mV at cathodic overpotential. All electrochemical measurements were recorded using an Autolab PGSTAT 302N potentiostat connected at one compartment cell with three electrodes: electrocatalyst designed cathode electrodes, a platinum anode electrode and Ag/AgCl, KCl reference electrode.

3. Results and discussion

3.1. Determination of potential value necessary in electrochemical deposition of AgNPs on Ti electrode for optimal electrocatalytic activity

In order to designed *Ti-AgNPs el* and *Ti/TiO$_2$NTs-AgNPs el* electrocatalysts, first, it is necessary to determinate the optimal potential value requested in *Ag NPs* electrodeposition process on Titanium electrode by chronoamperometry method.

Thereby, the different potential values were applied for 50 s started from -0.7 V up to -1 V vs. Ag/AgCl electrode, figure 2.

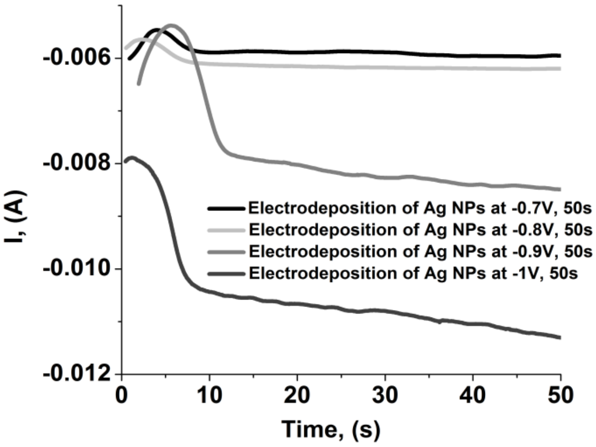

Fig. 2. Chronoaperometry curves for Ag NP electrodeposition at -0.7 V, -0.8V, -0.9V and -1 V for 50 s each, using AgNO$_3$ 0.1 M aqueous solution

In all cases, in the first five seconds the current increases, due to develop of silver nucleation process on substrate surface and then the current leads to steady stage, indicating that the Ag layer thickness grown and covered entire Ti surface. The current values became more electronegative with applied potential, leading to agglomeration of *Ag NPs* onto metallic substrate.

The distribution of Ag NPs onto Ti substrate was evaluated by the SEM image, illustrated in figure 3.

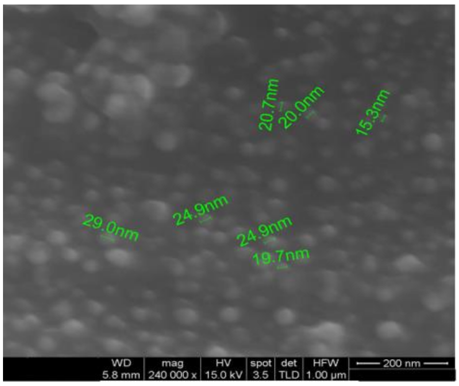

Fig. 3. SEM image of Ag NP electrodeposited on Ti substrate (Ti-AgNPs el. electrocatalyst) at -0.8 V

The surface morphology of *AgNPs electrodeposited* onto Ti substrate has a granular organization, with small size between 10 and 30 nm and these grains cover entire surface uniformly.

After electrodeposition of *AgNPs el* onto Ti electrodes, the electrocatalytic activity toward HER was measured in 0.1 M HCl solution using the LSV method to determine which potential value should be used to get the optimal electrocatalyst. For the following measurements, the electrocatalyst with the best catalytic behavior was chosen, and the optimal potential value was established.

In next figure (figure 4), the cathodic polarization curves expose the influence of the applied potential value on electrocatalytic activity toward HER for obtained *Ti-AgNPs el* electrocatalysts.

The overpotential of the hydrogen evolution reaction ($\eta H_2/2H^+$) was computed with next equation:

$$\eta_{H2/2H+} = E^{\circ}_{H2/2H+} - E_{WE}, \tag{1}$$

where E_{WE} represents the working electrode potential (V) and $E^{\circ}_{H2/2H+}$ represents the reversible hydrogen potential which was calculated with the relation: $E^{\circ}_{H2/2H+} = - 0.059 \cdot pH$ [46]. In our case, at a pH value of 0.95 for 0.1 M HCl solution and hydrogen partial pressure of 1, the $E^{\circ}_{H2/2H+}$ value is - 0.056 V vs. NHE.

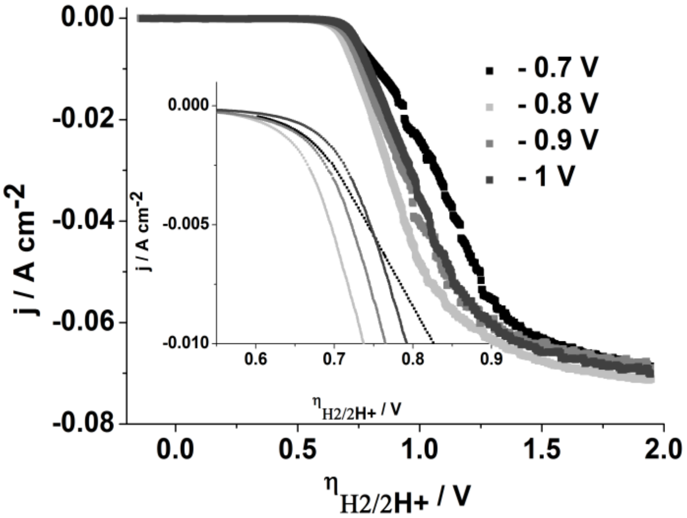

Fig. 4. Cathodic current vs. overpotential of the hydrogen evolution reaction recorded for Ti-AgNPs electrodeposited at different potential values for 50 s

According to the findings, the highest HER catalytic activity was observed when Ti-AgNPs were electrodeposited at -0.8 V for 50 s on a surface where proton reduction begins at a low overpotential of 0.62 V.

3.2. Morphologies and compositions of AgNPs chemical and electrochemical synthesized on Ti and Ti/TiO$_2$NTs supports

3.2.1. SEM images of the nanotubular titanium oxides with AgNPs deposited by chemical and electrochemical methods

Due to the fact that in this paper the main goal is to increases the surface aria of Ag electrocatalyst used for HER activity, the Ag was deposited onto modified Ti substrate with TiO_2 nanotubes by electrochemical and chemical methods.

Thereby, in next figures the SEM images of the Ag obtained by electrochemical and chemical methods onto TiO_2 NTs are depicted.

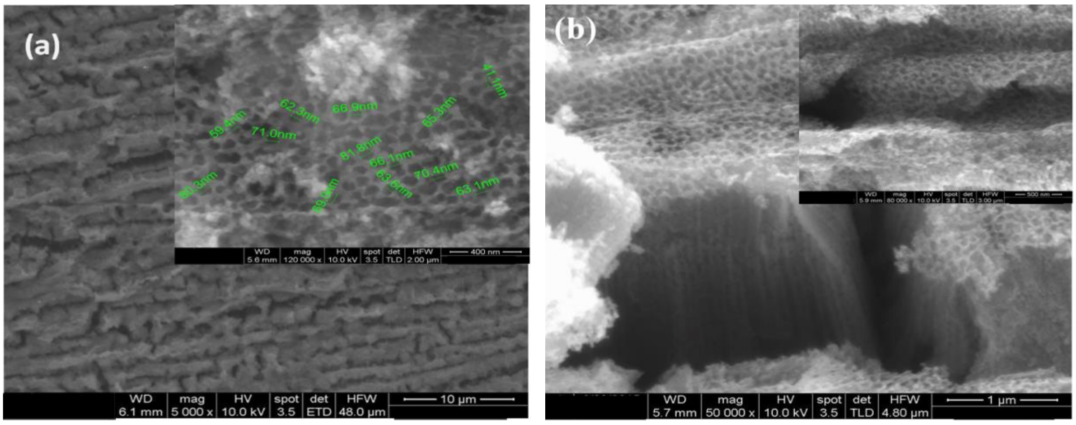

Fig. 5. SEM image of Ti/TiO$_2$NTs-AgNPs el electrocatalist for HER: (a) top view (b) in section view.

Like was already shown in figure 3, electrodeposited AgNPs have a granular organization around the TiO$_2$ nanotube. In figure 5a), from the top view of the *Ti/TiO$_2$NTs-AgNPs el* electrocatalist, AgNPs were electrodeposited on the TiO$_2$NTs walls and in some places appear agglomerations, which covering entire TiO$_2$NTs surface. The TiO$_2$NTs lined with electro-deposited AgNPs have the inner diameter between 40 and 82 nm and the wall thickness between 11 and 25 nm. The section view, figure 5b), shown that the AgNPs were electrodeposited lengthwise on TiO$_2$NTs, keeping in the same time the tubular structure.

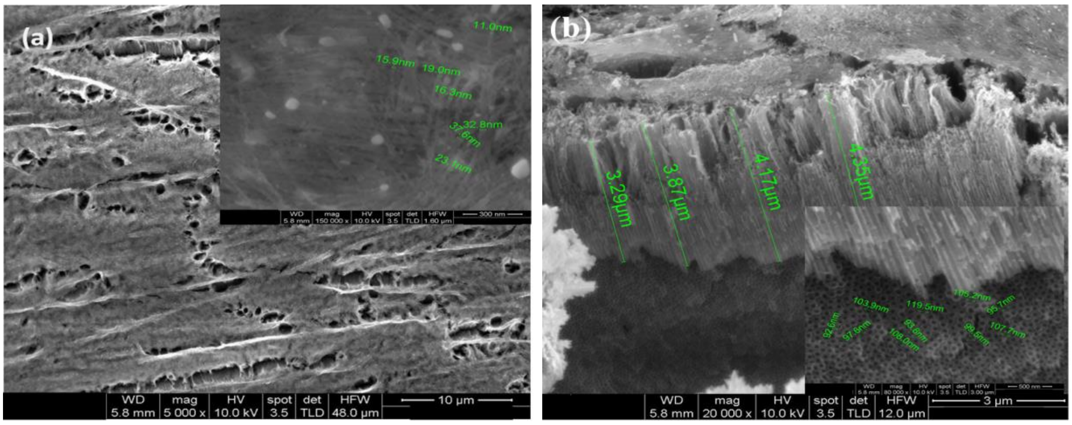

Fig. 6. SEM image of Ti/TiO$_2$NTs-AgNPs ch electrocatalist for HER: (a) top view (b) in section view.

On the other hand, in case of chemical method, figure 6a), AgNPs *ch* have a fibers type organization above TiO$_2$ nanotubes, covering entire surface. The diameter of Ag fibers is between 11 and 30 nm, and in some places AgNPs agglomerations are present with dimensions between 9 and 70 nm. From section view, figure 6b), was observed that these Ag nanofibers have surrounded entire surface of the nanotube on a length of about 4.4 μm. The outer diameter of TiO$_2$NTs covered with Ag nanofibers is between 90 and 120 nm, and the inner one is between 40 and 55 nm, smaller than in case of TiO$_2$NTs covered with electrodeposited AgNPs *el*.

3.2.2. EDAX results

The quantitative presence of AgNPs on both chemical and electrochemical catalysts was put in evidence by energy dispersive X-ray analysis (EDAX), figure 7.

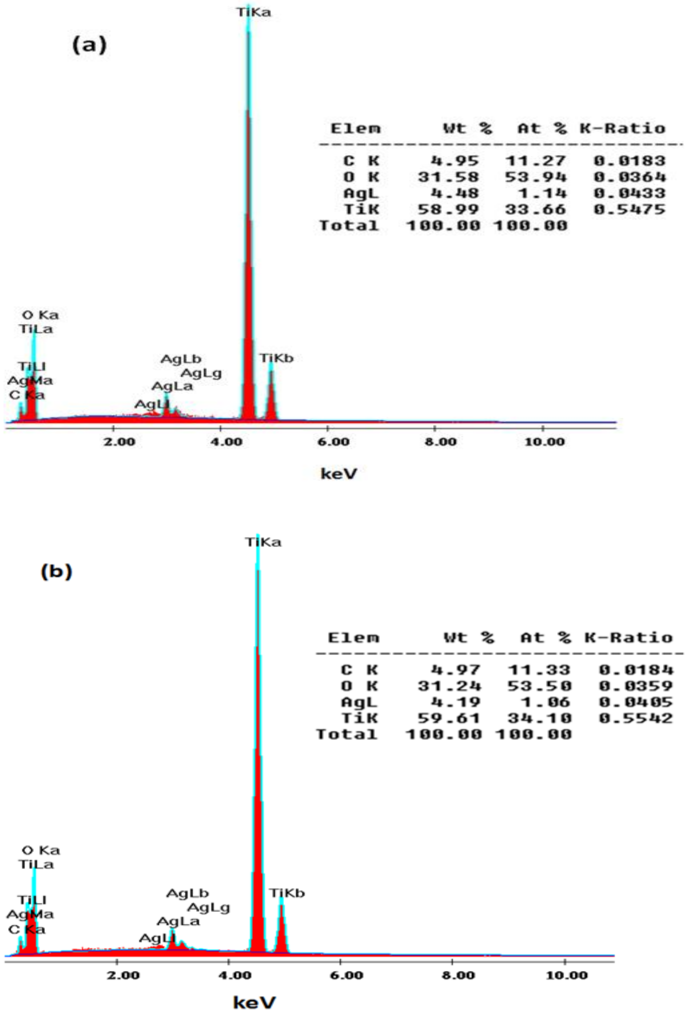

```
Elem      Wt %    At %  K-Ratio
-------------------------------
 C K      4.95   11.27   0.0183
 O K     31.58   53.94   0.0364
 AgL      4.48    1.14   0.0433
 TiK     58.99   33.66   0.5475
Total   100.00  100.00
```

```
Elem      Wt %    At %  K-Ratio
-------------------------------
 C K      4.97   11.33   0.0184
 O K     31.24   53.50   0.0359
 AgL      4.19    1.06   0.0405
 TiK     59.61   34.10   0.5542
Total   100.00  100.00
```

Fig. 7. EDAX examinations of (a) Ti/TiO$_2$NTs-AgNPs ch. and (b) Ti/TiO$_2$NTs-AgNPs el. electrocatalysts for HER

The EDAX spectra, figure 7 (a) and (b), reveal signals from Ti (~ 4.5 keV/Kα), Ag (~ 3 keV/Kα) and O (~ 0.7 keV/Kα) with different mass percentages, depending on the method used for deposit of AgNPs on the Ti/TiO$_2$NTs substrate. The content of AgNPs with fibers type organization (4.48 wt %), obtained by chemical method in presence of flour ions in the synthesis solution, is little bigger than that obtained by electrochemical method (4.19 wt %). This may indicate a penetration of F$^-$ ions into the oxide nanotube substrate, making the AgNPs precipitation easier.

3.3. Applications - electrocatalytic activity of Ti-AgNPs el, Ti-AgNPs ch, Ti/TiO$_2$NTs-AgNPs el, Ti/TiO$_2$NTs-AgNPs ch electrodes towards the HER

3.3.1. Cathodic polarization measurements

In order to evaluate the electrocatalytic activity of designed electrodes, the cathodic behavior was studied in 0.1 M HCl solution comparatively with the unmodified Ti electrode, using LSV method at a scan rate of 1.0 mV s^{-1}. In figures 8 (a) and (b) the cathodic polarization results were plotted at different scales in order to highlight the influence of the TiO$_2$ nanotubes presence and the type of synthesis method used for Ag nanoparticles deposited onto Ti substrate.

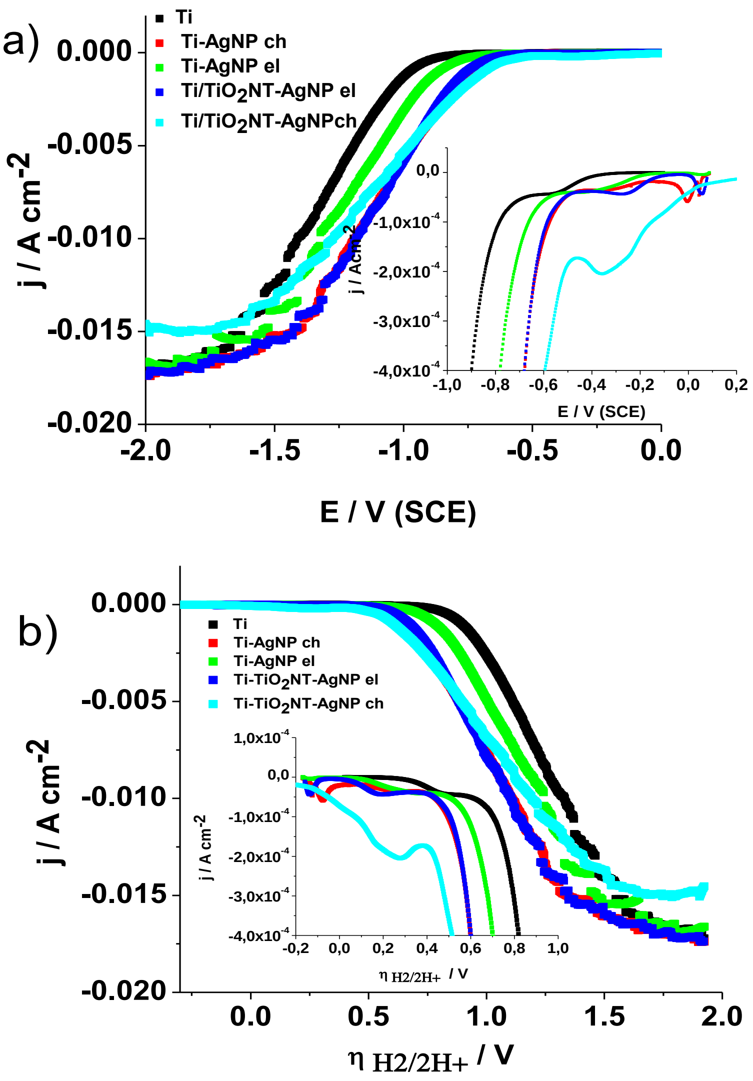

Fig. 8. Cathodic current vs. (a) electrode potential, E(SCE), and (b) overpotential of the hydrogen evolution reaction ($\eta H_2/2H^+$), recorded for untreated Ti, Ti-AgNPs el, Ti-AgNPs ch, Ti/TiO_2NTs-AgNPs el, Ti/TiO_2NTs-AgNPs ch electrodes, obtained in 0.1 M HCl solution (pH 0.95) at a scan rate of 1.0 mV·s^{-1}.

In Table 1 the reduction potential (E_c) and overpotential of the hydrogen evolution reaction ($\eta H_2/2H^+$) values were exhibited:

Table 1. The reduction potential and overpotential of the hydrogen evolution reaction values.

Electrocatalysts for HER	**E_c (V)**	**$\eta_{H2/2H+}$ (V)**
Ti	- 0.88	0.82
Ti-AgNPs ch	- 0.66	0.55
Ti-AgNPs el	- 0.74	0.75
Ti/TiO_2NTs-AgNPs ch	- 0.54	0.49
Ti/TiO_2NTs-AgNPs el	- 0.65	0.52

Cathodic polarization data revealed that the presence of AgNPs, obtained from both chemical and electrochemical deposition methods, leads to improve the catalytic activity of the Titanium electrode. The reduction potential for *Ti-AgNPs ch* electrocatalyst electrode has a less electronegative value (- 0.66 V) and a smaller overpotential values (0.55 V) compared with *Ti-AgNPs el* electrode. This proves that the AgNPs deposited method influences the catalytic properties of the final designed electrocatalysts, due to the fact that the deposited Ag layer has a different morphology which depends on the obtaining method, as was observed from SEM images. Moreover, the presence of TiO_2NTs onto the Ti substrate, before the AgNPs deposition, increases the hydrogen evolution reaction in both chemical and electrochemical deposition methods. The reduction potential values are higher and also, the overpotential values are smaller towards electrocatalysts designed without TiO_2 nanotubes. This behavior can be explained by the fact that the nanotubes presence leads to the enhancement of the contact surface of the catalyst, the Ag nanoparticles have been deposited both above and along TiO_2 nanotubes, according to SEM images. The best catalytic activity was achieved for Ag nanoparticles deposited by chemical method above/along TiO_2NTs template (*Ti/TiO₂NTs-AgNPs ch* electrocatalyst), which has a reduction potential by - 0.54 V and the lowest overpotential value by 0.49 V. This means that the fibers type organization of *AgNPs ch* above/along TiO_2 nanotubes improves the contact surface of the final catalyst, comparing to the granular organization of the Ag nanoparticles (*AgNPs el*) obtained by electrochemical deposition method. From SEM results was demonstrated that the walls of the TiO_2 nanotubes covered with Ag nano-fibers are thicker than those covered with Ag nano-grains, leading to a higher contact surface, as expected.

3.3.2. Electrochemical Impedance Spectroscopy

Other parameter used to evaluate the electrocatalytic activity of the designed electrocatalysts towards the HER was polarization resistance values (R_p) from EIS data. If the R_p have high values, then the catalytic activity of the designed electrocatalysts is smaller.

In Figure 9 the Nyquist plots, obtained in 0.1 M HCl solution and in the frequency range between 0.01 Hz to 100 kHz, are depicted for untreated Ti, *Ti-AgNPs el, Ti-AgNPs ch, Ti/TiO₂NTs-AgNPs el, Ti/TiO₂NTs-AgNPs ch* electrocatalysts.

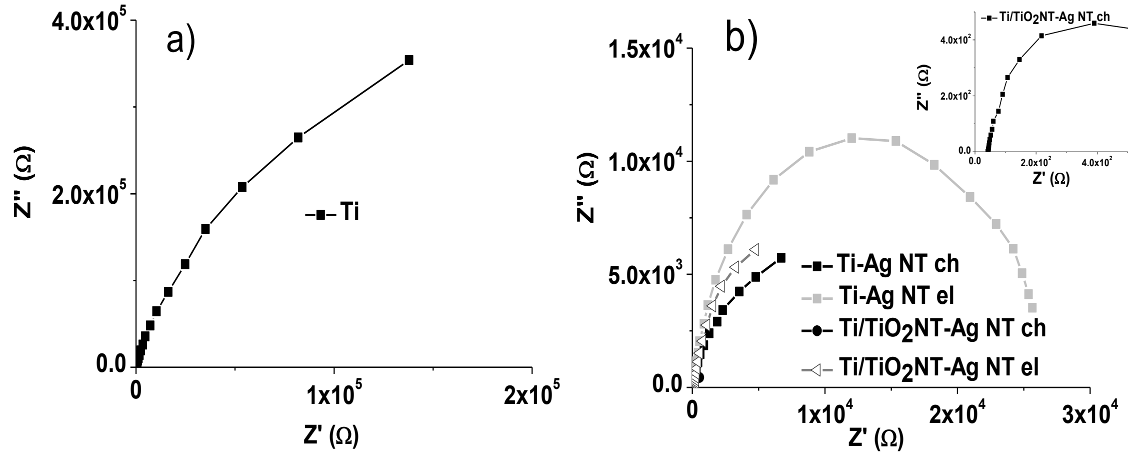

Fig. 9. Nyquist spectra for (a) untreated Ti and (b) Ti-AgNPs el, Ti-AgNPs ch, Ti/TiO₂NTs-AgNPs el, Ti/TiO₂NTs-AgNPs ch designed electrocatalysts.

The electrochemical parameters computed with Nova software from fitting EIS data are presented in Table 2. A Randles circuit [35] was used to fit the EIS data, which contains following parameters [35]: R_s - 0.1 M HCl electrolyte resistance; R_p - polarization resistance of the designed electrocatalysts/electrolyte interface with a constant phase element (CFE).

Table 2. Electrochemical parameters obtained from fitting of EIS data.

Electrocatalysts for HER	**R_s ($\Omega\cdot cm^2$)**	**R_p ($\Omega\cdot cm^2$)**	**CFE ($\Omega^{-1}\cdot cm^{-2}\cdot s^n$)**	**n**
Ti	327.34	$1.555\cdot10^6$	$10.23\cdot10^{-6}$	0.998
Ti-AgNPs ch	175.14	$14.649\cdot10^3$	$233.98\cdot10^{-6}$	0.997
Ti-AgNPs el	61.41	$26.803\cdot10^3$	$48.61\cdot10^{-6}$	0.998
Ti/TiO$_2$NTs-AgNPs ch	43.54	$1.553\cdot10^3$	$10.24\cdot10^{-3}$	0.999
Ti/TiO$_2$NTs-AgNPs el	225	$14.13\cdot10^3$	$1.126\cdot10^{-3}$	0.999

The EIS data reveal that the polarization resistance (R_p) values corresponding to electrocatalysts with Ag nanoparticles decreased with three order of magnitude than the untreated Ti electrode. As expected, the nanostructured modification treatment before the Ag NPs deposition enhances the catalytic activity of the final designed electrocatalysts. The smaller R_p value was recorded for *Ti/TiO$_2$NTs-AgNPs ch* electrocatalyst, these results being in accordance with the LSV data. In all cases the electrocatalysts displayed a pseudo-capacitive behavior, as resulted from n values.

4. Conclusions

Electrocatalysts for HER reaction have been designed by synthesizing of the Ag nanoparticles onto Titanium substrate with a fiber type organization using the chemical method and respectively, with a granular organization by the electrochemical deposition method.

Also, the active surface area of the AgNPs based electrocatalysts was enhanced by the anodization of the Titanium substrate and obtaining of self-organized TiO_2 nanotubes arrays, before the AgNPs deposition by both methods.

The influence of the AgNPs synthesized method and the TiO_2NTs presence on the electrocatalytic activity of *Ti-AgNPs el*, *Ti-AgNPs ch*, *Ti/TiO$_2$NTs-AgNPs el* and *Ti/TiO$_2$NTs-AgNPs ch* electrodes towards the HER was investigated. The presence of TiO_2NTs onto the Ti substrate, before the AgNPs deposition, increases the hydrogen evolution reaction in both chemical and electrochemical deposition methods.

The best electrocatalytic activity was found for the *Ti/TiO$_2$NTs-AgNPs ch* electrode with fibers type organization of *AgNPs ch* above/along TiO_2 nanotubes. This type of AgNPs organization leads to a higher contact surface in comparison to the granular organization of the Ag nanoparticles (*AgNPs el*) obtained by electrochemical deposition method.

References

[1] Y. Wang, L. M. Vu, T. Lu, C. Xu, Y. Liu, J. Z. Ou, Y. Li, ACS Appl Mater Interfaces 12(46), 51662 (2020); https://doi.org/10.1021/acsami.0c16039

[2] M. M. A. M. A. Aktar, A. Q. Al-Amin, Sustainable Production and Consumption 26, 770 (2021); https://doi.org/10.1016/j.spc.2020.12.029

[3] V. T. N. Lutfi N., Int. J. Hydrog. Energy., 16, 169 (1991); https://doi.org/10.1016/0360-3199(91)90001-Y

[4] V. T. N. Momirlana M., Int. J. Hydrog. Energy., 30, 795 (2005); https://doi.org/10.1016/j.ijhydene.2004.10.011

[5] A.-L. Schönauer, S. Glanz, International Journal of Hydrogen Energy, (2021).

[6] J. N. Armor, Catalysis Letters 101(3-4), 131 (2005); https://doi.org/10.1007/s10562-005-4877-3

[7] R. Ramachandran, R. K. Menon, International Journal of Hydrogen Energy 23(7), 593 (1998); https://doi.org/10.1016/S0360-3199(97)00112-2

[8] R. Kothari, D. P. Singh, V. V. Tyagi, S. K. Tyagi, Renewable & Sustainable Energy Reviews 16(4), 2337 (2012); https://doi.org/10.1016/j.rser.2012.01.002

[9] C. Gallert, A. Henning, J. Winter, Water Research 37(6), 1433 (2003); https://doi.org/10.1016/S0043-1354(02)00537-7

[10] R. Kothari, D. Buddhi, R. L. Sawhney, International Journal of Hydrogen Energy 30(3), 261 (2005); https://doi.org/10.1016/j.ijhydene.2004.03.030

[11] V. Mazanek, J. Luxa, S. Matejkova, J. Kucera, D. Sedmidubsky, M. Pumera, Z. Sofer, ACS Nano 13(2), 1574 (2019).

[12] X. Li, Z. Niu, J. Jiang, L. Ai, Journal of Materials Chemistry A 4(9), 3204 (2016); https://doi.org/10.1039/C6TA00223D

[13] Y. Wang, B. Ren, J. Zhen Ou, K. Xu, C. Yang, Y. Li, H. Zhang, Science Bulletin 66(12), 1228 (2021); https://doi.org/10.1016/j.scib.2021.02.007

[14] P. E. C. Bockris J.O.M., J. Electrochem. Soc., 99, 169 (1952); https://doi.org/10.1149/1.2779692

[15] C. Batchelor-Mcauley, C. E. Banks, A. O. Simm, T. G. J. Jones, R. G. Compton, Chemphyschem 7(5), 1081 (2006); https://doi.org/10.1002/cphc.200500571

[16] A. I. A. Bockris J.O.M., Huq A.K.M.S., , J. Phys. Chem. C, 61, 879 (1957); https://doi.org/10.1021/j150553a008

[17] L. G. I. Villuillas H.M., Gioda A.S., Macagno V.A.,, Electrochim Acta, 32, 1657 (1987); https://doi.org/10.1016/0013-4686(87)90021-1

[18] C. Lupi, A. Dell'era, M. Pasquali, International Journal of Hydrogen Energy 34(5), 2101 (2009); https://doi.org/10.1016/j.ijhydene.2009.01.015

[19] M. Cappadonia, S. Krause, U. Stimming, Electrochimica Acta 42(5), 841 (1997); https://doi.org/10.1016/S0013-4686(96)00332-5

[20] D. Marin, F. Mendicuti, C. Teijeiro, Journal of Chemical Education 71(11), A277 (1994); https://doi.org/10.1021/ed071pA277

[21] A. A. Gurten, K. Kayakirilmaz, B. Yazici, M. Erbil, International Journal of Hydrogen Energy 28(10), 1083 (2003).

[22] J. Xie, H. Zhang, S. Li, R. Wang, X. Sun, M. Zhou, J. Zhou, X. W. Lou, Y. Xie, Adv Mater 25(40), 5807 (2013); https://doi.org/10.1002/adma.201302685

[23] Z. C. H. Li, C.K. Tsang, Z. Li, X. Ran, C. Lee, B. Pan, J. Mater. Chem. A 2 (2014), 229; https://doi.org/10.1039/C3TA13963H

[24] Z. Liu, X. Zhang, B. Wang, M. Xia, S. Gao, X. Liu, A. Zavabeti, J. Z. Ou, K. Kalantar-Zadeh, Y. Wang, The Journal of Physical Chemistry C 122(24), 12589 (2018); https://doi.org/10.1021/acs.jpcc.8b01678

[25] Q. B. Deng, M. Smetanin, J. Weissmuller, Journal of Catalysis 309, 351 (2014); https://doi.org/10.1016/j.jcat.2013.10.008

[26] Y. Wang, B. J. Carey, W. Zhang, A. F. Chrimes, L. Chen, K. Kalantar-Zadeh, J. Z. Ou, T. Daeneke, The Journal of Physical Chemistry C 120(4), 2447 (2016); https://doi.org/10.1021/acs.jpcc.5b10939

[27] L. Zheng, F. Teng, X. Ye, H. Zheng, X. Fang, Advanced Energy Materials 10(1), 1902355 (2020); https://doi.org/10.1002/aenm.201902355

[28] K. M. Emran, Int. J. Electrochem. Sci 15, 4218 (2020); https://doi.org/10.20964/2020.05.02

[29] U. Lačnjevac, R. Vasilić, A. Dobrota, S. Đurđić, O. Tomanec, R. Zbořil, S. Mohajernia, N. T. Nguyen, N. Skorodumova, D. Manojlović, N. Elezović, I. Pašti, P. Schmuki, Journal of Materials Chemistry A 8(43), 22773 (2020); https://doi.org/10.1039/D0TA07492F

[30] H. Song, X. Qiu, F. Li, Electrochimica Acta 53(10), 3708 (2008); https://doi.org/10.1016/j.electacta.2007.11.080

[31] M. Tanveer, A. Habib, M. Bilal Khan, Current Nanoscience 9(3), 351 (2013); https://doi.org/10.2174/1573413711309030010

[32] M. Ye, X. Xin, C. Lin, Z. Lin, Nano letters 11(8), 3214 (2011);

https://doi.org/10.1021/nl2014845
[33] N. Liu, C. Schneider, D. Freitag, M. Hartmann, U. Venkatesan, J. MüLler, E. Spiecker, P. Schmuki, Nano letters 14(6), 3309 (2014); https://doi.org/10.1021/nl500710j
[34] L. Taveira, J. Macak, H. Tsuchiya, L. Dick, P. Schmuki, Journal of the Electrochemical Society 152(10), B405 (2005); https://doi.org/10.1149/1.2008980
[35] M. Mîndroiu, C. Pirvu, R. Ion, I. Demetrescu, Electrochimica Acta 56(1), 193 (2010); https://doi.org/10.1016/j.electacta.2010.08.100
[36] K. M. Alaqad, T. A. Kandiel, C. Basheer, International Journal of Hydrogen Energy 47(4), 2366 (2022); https://doi.org/10.1016/j.ijhydene.2021.10.159
[37] P. Frontera, A. Malara, S. Stelitano, S. G. Leonardi, A. Bonavita, E. Fazio, P. Antonucci, G. Neri, F. Neri, S. Santangelo, Materials Chemistry and Physics 170, 129 (2016); https://doi.org/10.1016/j.matchemphys.2015.12.030
[38] J. M. Macak, P. Schmuki, Electrochimica Acta 52(3), 1258 (2006); https://doi.org/10.1016/j.electacta.2006.07.021
[39] I. Paramasivam, J. Macak, P. Schmuki, Electrochemistry Communications 10(1), 71 (2008); https://doi.org/10.1016/j.elecom.2007.11.001
[40] J. M. Macak, B. G. Gong, M. Hueppe, P. Schmuki, Advanced Materials 19(19), 3027 (2007); https://doi.org/10.1002/adma.200602549
[41] R. Zazpe, H. Sopha, J. Prikryl, M. Krbal, J. Mistrik, F. Dvorak, L. Hromádko, J. Macak, Nanoscale 10(35), 16601 (2018); https://doi.org/10.1039/C8NR02418A
[42] L. Xie, L. Wang, W. Zhao, S. Liu, W. Huang, Q. Zhao, Nature communications 12(1), 1 (2021); https://doi.org/10.1038/s41467-021-25381-1
[43] W. F. Chen, K. Sasaki, C. Ma, A. I. Frenkel, N. Marinkovic, J. T. Muckerman, Y. Zhu, R. R. Adzic, Angewandte Chemie International Edition 51(25), 6131 (2012); https://doi.org/10.1002/anie.201200699
[44] J. E. Yoo, K. Lee, M. Altomare, E. Selli, P. Schmuki, Angewandte Chemie International Edition 52(29), 7514 (2013); https://doi.org/10.1002/anie.201302525
[45] J. M. Macak, T. Kohoutek, L. Wang, R. Beranek, Nanoscale 5(20), 9541 (2013); https://doi.org/10.1039/c3nr03014h
[46] M. A. Amin, S. A. Fadlallah, G. S. Alosaimi, international journal of hydrogen energy 39(34), 19519 (2014); https://doi.org/10.1016/j.ijhydene.2014.09.100
[47] K. M. Alaqad, T. A. Kandiel, C. Basheer, ChemCatChem 12(21), 5411 (2020); https://doi.org/10.1002/cctc.202000828
[48] Z.-J. Jiang, C.-Y. Liu, L.-W. Sun, The Journal of Physical Chemistry B 109(5), 1730 (2005); https://doi.org/10.1021/jp046032g
[49] J. R. Morones, J. L. Elechiguerra, A. Camacho, K. Holt, J. B. Kouri, J. T. Ramírez, M. J. Yacaman, Nanotechnology 16(10), 2346 (2005); https://doi.org/10.1088/0957-4484/16/10/059
[50] Y. Wang, J. Zhou, T. Wang, Materials Letters 62(12-13), 1937 (2008); https://doi.org/10.1016/j.matlet.2007.10.045
[51] C. Wen, A. Yin, W.-L. Dai, Applied Catalysis B: Environmental 160, 730 (2014); https://doi.org/10.1016/j.apcatb.2014.06.016
[52] T.-C. Pan, S.-H. Wang, Y.-S. Lai, J.-M. Jehng, S.-J. Huang, Applied surface science 296, 189 (2014); https://doi.org/10.1016/j.apsusc.2014.01.077